Encycl. Phys.Sci.& Technol. 2001
Academic Press

ION BEAMS FOR MATERIALS ANALYSIS

David D. Cohen, Roger Bird, Nick Dytlewski and Rainer Siegele

Australian Nuclear Science and Technology Organisation
Private Mailbag 1, Menai, NSW, 2234, Australia.

I. Equipment Requirements
II. Principles and Examples
III. Applications

GLOSSARY

Blocking: Reduction of detector signal rate when aligned with a crystal axis or plane.
Channeling: Guided trajectory of incident ions between crystal axes or planes.
Collision cascade: Series of atom-atom collisions initiated by an ion-atom collision.
Cross section: Effective area presented by each atom or nucleus for a specific type of interaction with an incoming ion.
lmplantation: Addition of controlled concentration of atoms to a near-surface layer by irradiation with a known dose of incident ions.
Shadowing: Reduction in probability of ion interactions with atoms that lie behind a surface atom in the direction of the incident ion beam.
Sputter profiling: Determination of variation in isotope concentrations with depth by analysis as a function of time during sputtering.
Sputtering: Emission of atoms or ions following a collision of an energetic ion with surface atoms.
Stopping power: Rate of energy loss of incident ion as it penetrates below the surface of a sample.

Ion beam analysis (IBA) involves the irradiation of a sample by a beam of ions and the detection of one or more types of emitted radiation or particles that convey information on the sample composition and structure. At low energies (1-10 keV), O, Ne, or other heavy ion beams may be scattered from surface atoms or may cause removal of neutral, ionized, or excited atoms from the surface layer. At high energies (> 100 keV) proton, alpha, or heavier ions scatter from the nuclei of sample atoms or cause X-ray, γ-ray, ion, or neutron emission from interactions or even sample atom recoil at depths of up to many micrometers. These processes are used as the basis for four types of sample analysis:

1. composition analysis - determination of isotopic or elemental concentrations from the observed radiation yield;
2. depth profiling - from the time dependence of sputter induced signals or from the dependence of radiation yield on the energy of incident or emitted radiation or particles;
3. structure analysis - from the angular dependence of radiation intensities; and
4. microprobe analysis - using a beam of 1 μm in diameter or less scanned across a sample in one or two dimensions to obtain a spatial distribution.

IBA is a suite of techniques that may either be used singly for specialized applications or in combinations to obtain more extensive and detailed information of atom concentrations.

The principles of ion beam interactions have been known for many years, but there is still some work to be done to extend data banks, optimize experimental conditions for each type of analysis, and improve the understanding of ion-atom and atom-atom interactions. However, IBA is already

widely used, with a rapidly increasing number of facilities providing key information in many areas of science and technology. The general area of ion beam analysis has been adequately summarised by the ongoing IBA international conference series held every two years the proceedings of which have been published regularly, see for example IBA 1998 and the references therein.

I. Equipment Requirements

Except for specialised external beam analysis, IBA is carried out in a vacuum. At low to medium ion energies, a typical system uses an ion gun, a beam analyzer, a sample mount, a quadrupole mass analyzer or an electrostatic energy analyzer, and an ion detector mounted in a chamber at a pressure of 0.01 mPa or less. For neutral atom or photon spectrometry, special analysis and detection techniques are used [Bird and Williams, 1989]. A complete system may be purchased, but it is often assembled from components selected to provide the performance required for specific applications. The secondary ion microscope uses a broad diameter incident beam and imaging optics to record the spatial distribution of secondary ions with a selected mass. The secondary ion microprobe (SIMP) uses sophisticated equipment for mass analysis, focusing and scanning the incident ion beam (1 μm in diameter or less). Detector signals are recorded as a function of sweep time to provide an isotope or element concentration as a function of position on the sample. Additional equipment may be included for electron beam and other surface analysis techniques that give information complementary to that from IBA.

At high energies, an ion source and MV accelerator are followed by a magnetic analyzer with feedback controls to maintain the accelerator voltage constant to within 0. 1 to 1 kV. The ion beam can usually be deflected in one of a number of target chambers (operating at pressures from 0.1 to 0.01 mPa or lower) that have been set up for various types of IBA [Bird and Williams, 1989]. Semiconductor, gas or scintillation detectors record the energy of the particles or radiation emitted; magnetic or electrostatic analyzers may also be used. A thin absorber foil can be placed in front of a detector to remove the lowest energy particles and radiation. Such a facility may occupy a large laboratory and cost several million dollars but many accelerators, installed originally for nuclear physics research, are now used partially or exclusively for IBA. A growing number of laboratories have purpose-designed accelerators operating full time for IBA. These machines typically have terminal voltages around or below 3 MV.

Ion beams from accelerators are typically 1 to 10 mm in diameter. Recently, however, considerable research has been done with focussed ion beams with beam diameters as low as 1 μm [Breese et al, 1996]. These beams are generally focused by several magnetic quadrupoles. Typically, proton or alpha particle beams have been used with energies between 1 and 3 MeV/amu and beam spot sizes between 1 and 10 μm diameter [Legge and Jamieson, 1991]. Although the current smallest focussed spot for proton beams is around 0.3 μm obtained using the Oxford quadrupole triplet at the National University of Singapore [Watt et al, 1998].

There are now over 50 proton nuclear microprobes system world wide. They are also available commercially and include special beam focusing and scanning equipment plus multidimensional data recording [Vis et al, 1990]. The ion beam methods, particle induced X-ray emission (PIXE), particle induced gamma ray emission (PIGME), Rutherford backscattering (RBS), nuclear reaction analysis (NRA), and channeling can all be used to obtain spatial distributions of one or more isotopes or elements [Duggan et al,

1991; Moschini and Valkovic, 1996]. The minimum beam diameter and maximum beam current are dependent on the brightness of the ion source and energy stability of the accelerator. A spatial resolution of 1 μm or better can be obtained with a beam current of 100 pA. Even at this current, rapid scanning may be needed to minimize damage to some types of sample. The short working distance in a nuclear microprobe system (< 20 cm) makes it difficult to position large detectors near the sample for high counting efficiency. Scanning Transmission Ion Microscopy (STIM) requires much lower beam currents and utilizes forward ion scattering or ion induced secondary electrons to study the structure of ~100 nm thick samples with a spatial resolution of ~100 nm [Legge and Jamieson, 1991].

Depth profiling at low ion energies makes use of the sputter removal of surface atoms at rates up to ~5 nm minute^{-1} depending on the incident ion current [Feldman et al, 1986]. The beam is scanned over an area larger than that to be analyzed and electronic gating of detector signals prevents acceptance of those generated while the beam is close to the walls of the sputter pit that is created. Recording of detector signals as a function of time or dose then gives a depth profile (usually for one isotope or element at a time). At high ion beam energies, nondestructive depth profiling, with a depth resolution of 1-100 nm, is an intrinsic capability of many ion beam techniques - the resolution depending on the technique. Resonance profiling with a resolution of ~1 nm is possible for some light isotopes and this is best done using an automatic beam-energy modulation system [Deconninck, 1978].

Structure studies exploit the effects of shadowing at low energies or channeling and blocking at high energies [Feldman et al, 1982]. These require a well-collimated beam with a divergence of <0.1° FWHM (for example, using l-mm-diameter apertures spaced by several meters). A precision goniometer is also needed to position the sample to this accuracy in two or preferably three, angular directions.

An external beam of >2 MeV/amu of protons or helium ions can be produced by allowing them to pass from the vacuum into air or a helium atmosphere through a thin foil (<5 μm of metal or plastic). Although there is significant energy loss in the foil, the protons or helium ions can still travel many centimeters in air or helium and irradiate a sample for IBA purposes. This is useful for the study of samples that are too large, fragile, or valuable to be mounted within a vacuum chamber such as paintings or objects of art.

II. Principles and Examples

In an ion-atom collision, the energy of the scattered or product ion is given by:

$$E_p = XE_T\left[\cos\theta + Y/\left(X^2 - \sin^2\theta\right)^{1/2}\right]^2 \tag{1}$$

while the energy of the recoil atom is given by:

$$E_r = W\ E_T\left[\cos\phi + \left(V/X - \sin^2\phi\right)^{1/2}\right]^2 \tag{2}$$

where $W = m_i\, m_r\, E_i/E_T\, m$; $V = m_p\, m_r\, (l + m_i\, Q\, /\, m_a\, E_T)\, /\, m$; $X = m_I\, m_p\, E_i\, /\, E_T\, m$; $Y = m_a\, m_r\, (l + m_i\, Q\, /\, m_a\, E_T)\, /\, m$; $E_T = E_i + Q$; $m = (m_i + m_a)(m_p + m_r)$; θ is the product angle and ϕ is the recoil angle relative to the incident beam direction; E is energy and m is atomic mass with subscripts i = incident ion, p = product ion, a = target atom, and r = recoil atom; and Q is the energy balance that is zero for elastic scattering.

At low energies, collisions with atoms at the surface of the sample are most important, whereas at higher energies, an ion may penetrate to depths of many micrometers but loses energy as it does so. Electrons associated with the incident ion and sample

atoms may be excited or removed during ion-atom collisions, leading to gradual energy loss by the incident ion and neutralization, charge exchange, photon emission, etc. At high energies, scattering involves nucleus-nucleus collisions that also obey Eqs. (1) and (2). The probability for each specific type of interaction is represented by the cross section (dσ/ dΩ) and the interaction yield is given by

$$Y_p = N_i \; e \; d\Omega \int_{E_i}^{0} \left[(d\sigma / d\Omega) / S \right] dE \qquad (3)$$

where $d\Omega$ is the detector solid angle and S is the rate of energy loss (eV per atom cm^{-2}), which is more important in ion-atom interactions than the physical distance traveled by an ion. The relative magnitudes of cross sections for some high-energy interactions are shown in Fig. 1 as a function of the atomic number of the target atoms.

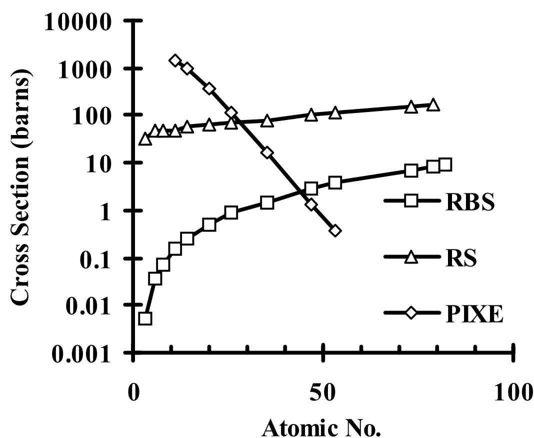

Fig. 1. Comparison of cross sections for Rutherford backscattering (RBS), recoil spectrometry (RS) and K shell PIXE.

It compares the cross sections for Rutherford backscattering (RBS) of 2 MeV helium ions (170°), for 2.5 MeV PIXE and for recoil spectrometry (RS) using a 65 MeV iodine beam (45°) for a range of targets with atomic numbers spanning the periodic table. The figure demonstrates the need to tailor the ion beam to the analysis required. K shell PIXE provides little depth information, has a larger cross section for the lighter elements below calcium but poorer sensitivity than RBS and RS for heavy elements above zirconium.

Recoil spectrometry with 65 MeV iodine beams at 45° has at least an order of magnitude larger cross section and hence better sensitivity than 2 MeV helium RBS at 170° for most elements across the periodic table. For the lighter elements such as carbon and oxygen this difference reaches two orders of magnitude. RBS is most useful in elemental profiling when the element being profiled is heavier than the matrix elements themselves and falls down badly when profiling light elements in a heavy matrix.

A. SCATTERING

The energy spectrum of ions scattered from atoms consists of a peak for each isotope present (Fig. 2). It is thus a mass spectrum with a nonlinear mass scale [Eq. (1)] and peak heights determined by Eq. (3). This type of spectrum is observed in low-energy ion scattering (LEIS) for which tabulated values or approximate expressions can be used for the cross section and neutralization probability [Benninghoven et al, 1988]. For example, rare gas ions have high neutralization probabilities and do not survive as ions beyond the first layer of atoms. They are, therefore, ideal probes for studying surface atom densities and surface structure (by exploiting shadowing and multiple collision effects) in materials such as catalysts, adsorbates, metallic glasses, and unusual alloys. Alkali and alkali metal ions have low neutralization probabilities and may produce scattering spectra with low-energy tails to each mass peak that arise from subsurface scattering. The tails increase as the incident energy is increased.

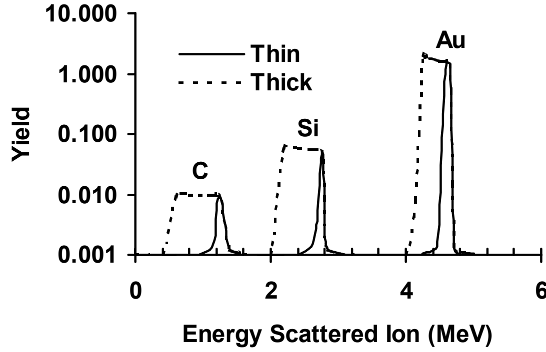

Fig. 2. Energy spectrum of ions scattered from surface atoms (full curve) and from atoms in a thin layer (dashed curve).

At high energies, the probability of scattering is given by the Rutherford backscattering (RBS) cross section, which has an analytical form that can be used for accurate calculation of atomic concentrations from observed scattering yields [Chu et al, 1978; Tesmer and Nastasi, 1995].

$$\frac{d\sigma}{d\Omega} = \left(\frac{Z_1 Z_2 e^2}{4E}\right)^2 \frac{4}{\sin^4}\theta \frac{\left\{\left[1-\left((M_1/M_2)\sin\theta\right)^2\right]^{1/2} + \cos\theta^2\right\}}{\left[1-\left((M_1/M_2)\sin\theta\right)^2\right]^{1/2}} \tag{4}$$

Non-Rutherford cross sections are observed in cases such as proton scattering from light elements such as oxygen [Cohen and Rose, 1992]. It is therefore customary in RBS to use 2 MeV He ions to avoid non-Rutherford effects. Each RBS mass peak is extended toward low energies by an amount dependent on the sample thickness and the rate of ion energy loss (dashed curves in Fig. 2). The shape of each segment of the spectrum can be used to derive the depth dependence of concentration of one isotope by using Eqs. (2) and (3). The depth scale is given approximately by

$$d = -\left[\left(dE_p / dE_i\right)S_i / \sin\alpha + S_p / \sin\beta\right]\Delta E_p \tag{5}$$

where ΔE_p is the difference in product energy at the surface and at depth d and α and β are the angles of beam and detector relative to the plane of the sample surface. The mass resolution is best at back angles near 180°, but the count rate is then lowest. A detector angle near 90° is sometimes used for higher count rates and good depth resolution (low values of α or β). This is a non-destructive method for depth profiling that is used extensively in studying thin films, multi-layer devices, the effects of ion implantation, diffusion, radiation damage, and other near-surface phenomena.

B. ELASTIC RECOIL DETECTION ANALYSIS

Elastic recoil detection analysis (ERDA) exploits target atom recoil in the forward direction (for example, 5° to 45°) following an interaction with a heavier high energy incident ion. Atoms that are lighter than the incident ion recoil with higher energy than that of forward scattered ions and are therefore easier to detect. ERDA is thus a unique method for determining and depth profiling light isotopes in the presence of heavier elements. For example, H can be profiled using an incident helium beam, and isotopes from Li to Zr can be profiled using a 100 MeV incident iodine beam. Ion beams from alphas to gold with energies in the range 0.3 to 2 MeV/amu are typically used depending on the energies available from the particle accelerators [Tirira et al, 1996].

More recently, multi-parameter detection systems have been employed with ERDA [Hult et al, 1995]. As well as an energy detection system, two timing mirrors are used to obtain a time of flight spectrum which is combined with the energy spectrum to form a two dimensional plot [Maritn et al 1994].

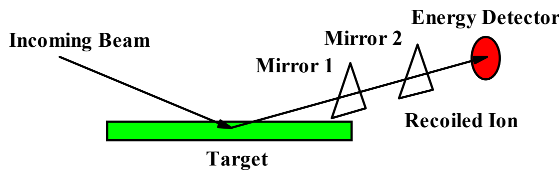

Fig. 3. Schematic of the recoil time of flight target and detection system.

A schematic of a forward recoil time of flight system is shown in Fig. 3. Heavy ions from the accelerator impinge on the target at an angle of between 5 and 45 degrees and recoiled particles are detected at a reaction angle of less than 90 degrees to the incoming beam by two electrostatic timing mirrors (typically 30-100 cm apart) and an ion implanted surface barrier energy detector. The start and stop timing mirrors are usually thin carbon foils (5-30 $\mu g/cm^2$) which generate a secondary electron timing signal detected by a set of microchannel plates. The overall timing resolution of the mirror system is typically less than 350 ps. This is more than adequate for measuring recoiled ion flight times of tens of nanoseconds over 30 cm or more. A typical 2D spectrum from such a system is shown in Fig. 4 for a thin TiO_2 layer on silicon. The recoil time of flight (ToF) spectrum is plotted against the energy spectrum producing a "boomerang" for each element from which the depth profiles can be obtained [Tirira et al, 1996]. The near surface regions are to the right (high energy) end of the boomerang to larger and larger depths as you slide down the boomerang to lower recoil energies. Short boomerangs, like the O and Ti in Figure 4, represent thin layer on the surface. For most practical situations the energy detector resolution dominates the ultimate depth resolution obtained even when, straggling, roughness and multiple scattering in the timing foils and the target materials are considered [Whitlow et al, 1991].

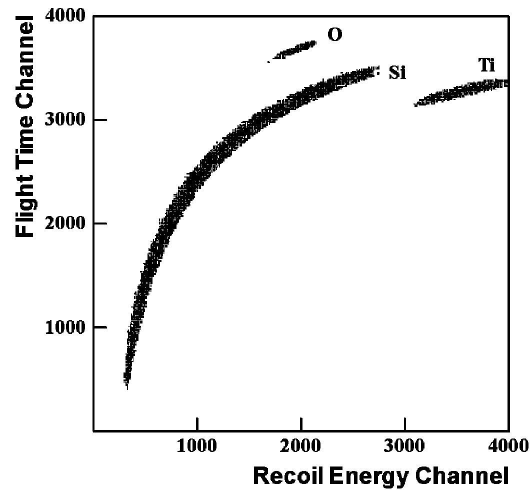

Fig. 4 Thin 100 nm TiO_2 layer on silicon spectrum for RToF using 77 MeV iodine beams.

C. CHANNELING

Channeling is most often used during RBS measurements on crystalline materials, although it is also used with other high-energy IBA measurements [Feldman et al, 1982]. The probability of scattering from subsurface atoms in a crystal is reduced by at least an order of magnitude for ions incident along the direction of a row or plane. Interactions with impurity atoms are also reduced if they occupy substitutional sites but not if they are interstitial. A typical RBS channeling measurement, at a scattered energy corresponding to a depth (*d*) is shown in Fig. 5. The scattering rate is plotted as a function of the angle of orientation of the sample relative to the direction of the incident beam. The figure shows the count rate (a) for a non channeling (random) orientation, the reduced yield (b) for a channeled direction, the further reduction in yield (c) when the detector is placed in a blocking direction, and the increased yield (e) for scattering from interstitial atoms. Channeling is a powerful technique for studying the degree of crystallinity of a sample, atom vibrations, defect and impurity atom locations, epitaxial layers, strained superlattices and many other topics requiring

structural information [Bird and Williams, 1989].

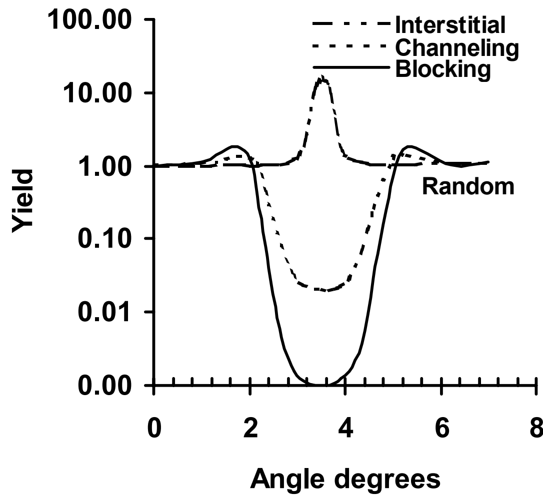

Fig. 5. The angle dependence of RBS yield from atoms in a crystal at a depth (d) below the sample surface (see text description).

D. SPUTTERING

A beam of O, Ne, Ar, or other heavy ions at 1-10 keV initiates collision cascades that result in the ejection of up to 20 surface atoms or ions per incident ion. Either positive or negative ion emission can be used in secondary ion mass spectrometry (SIMS) [Benninghoven, 1988]. which is a very sensitive method for measuring atomic concentrations. Any element can be detected with detection limits as low as 10^{-9} gg^{-1} in favourable cases. However, the sensitivity varies by up to two orders of magnitude for different elements in the same substrate or one element in different substrates. A beam of reactive gas ions (for example, O) gives a high and relatively uniform yield of positive ions from many elements, whereas a Cs beam gives good negative ion yields from electro-negative elements. SIMS is thus a powerful technique for studying traces of material, isotope ratios, etc. but quantitative analysis is only possible under carefully controlled conditions and when suitable calibration samples are available.

Neutral sputtered atoms can be ionized by laser or electron beams, or in plasma, or discharge cells to allow mass and energy analysis. Neutral yields are high and similar for most elements, so this is a valuable addition to other sputter techniques. Photon emission by excited atoms or ions is also useful, especially for the study of chemical bonding of surface atoms [Feldman et al, 1986].

Sputter profiling uses the ion beam techniques described previously or independent electron or laser probes to analyze the freshly exposed surface. The depth resolution depends on the escape depth of the radiation detected (usually 0.1 to 1 nm) and the effects of ion beam induced atomic mixing and micro-roughness. Other processes, such as ion implantation, preferential sputtering, and redeposition of sputtered material, can also affect both the local composition and the sensitivity so that quantitative interpretation of results may be difficult. Nevertheless, very sensitive analysis can be carried out to depths of many micrometers and can provide valuable information for many topics.

E. X-RAY EMISSION

Particle-induced X-ray emission (PIXE) follows ionization and atomic excitation caused by passage of an energetic ion through matter. PIXE yields from a thin sample exposed to an ion beam can be calculated from Eq. (3) and used to derive absolute concentrations from observed X-ray intensities [Bird and Williams, 1989]. For a thick sample, two integrations must be introduced to allow for the dependence of the cross section on ion energy (which decreases as the ion penetrates the sample) and the attenuation of the X-rays as they emerge from within the sample:

$$Y_x = N_i N_a e\, d\Omega \int_{E_1}^{0} \left[(d\sigma_x / d\Omega) T / S_i \right] dE \tag{6}$$

where the transmission is

$$T = \exp - \int_{E_1}^{E} \left(\mu \sin\alpha / S_i \sin\beta \right) dE \tag{7}$$

N_i is the number of incident ions and N_a is the number of target atoms per cm^2, and μ is the X-ray mass attenuation coefficient. Additional attenuation terms must be introduced to allow for any filters and other absorbers between the sample and the active volume of the detector. The effects of attenuation are most important for low X-ray energies and limit the precision that can be achieved for light elements (Z < 15). On the other hand, special absorbers can be used to preferentially attenuate high-intensity X-rays and allow higher ion currents to be used in the determination of trace elements. Other factors that must be considered during spectrum analysis include multiple X-ray lines, sum and escape peaks, non-Gaussian peak shapes, and various contributions to the background continuum [Bird and Williams, 1989]. A number of computer packages are available for analysis of thick sample spectra, and verification of the results using standard samples is always desirable.

Protons at 2 to 3 MeV are most often used for PIXE measurements and detection limits < 10 $\mu g g^{-1}$ are observed for 20 < Z < 40 (K X-rays) or 60 < Z < 90 (L X-rays). However, the L X-rays are often difficult to resolve from K X-rays with similar energies from lighter elements. The main attractions of PIXE are the high sensitivity, including very high absolute sensitivity (< 10^{-12} g), and its versatility for non-destructive multi-element analysis, and it is widely used for studies of minerals, air pollution, biomedicine, archaeology. etc.

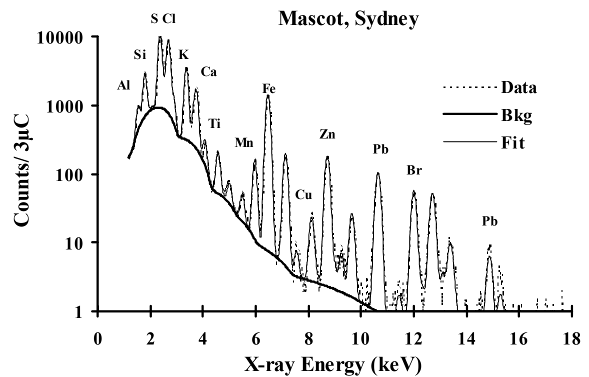

Fig. 6. Typical PIXE spectrum for aerosol filter collected at Mascot in Sydney, Australia showing a range of elements from Al to Pb present in 2.5 µm diameter atmospheric dust particles. Taken using 2.6 MeV protons and a standard Si(Li) detector.

F. GAMMA-RAY EMISSION

Particle-induced γ-ray emission (PIGME) follows the excitation of nuclear levels by incident ion beams. Gamma-ray energies and intensities are therefore isotope rather than element specific, although the same gamma ray may sometimes result from different reactions in different target isotopes [Deconninck, G., 1978]. The intensities are highest for light ion (^1H, ^2D, ^3T, ^3He, ^4He) irradiation of light isotopes (Z < 15), especially for beam energies less than 3 MeV. At higher energies, inelastic scattering excites gamma-ray emission in most isotopes. Observed yields can be calculated from Eq. (5) but without the attenuation term, which is negligible for the gamma-ray energies usually used (>100 keV). Absolute isotopic concentrations can be calculated provided that the production cross sections are accurately determined for the experimental conditions used. Li, Be, F, Na. and AI can be determined in thick samples with a sensitivity of 10 $\mu g\ g^{-1}$ or less using a 2-3 MeV proton or alpha beam [Bird and Williams, 1989]. A major use of PIGME is to extend PIXE analysis to include a number of light elements and can be carried out simultaneously with other

measurements by including other detection systems.

Many gamma-ray producing reactions have narrow resonant cross-section peaks that can be exploited for high-sensitivity and selectivity studies of thin layers, including depth profiling. If the beam energy is that of the resonance maximum, a high yield of gamma rays is produced in a layer within ~1 nm from the sample surface. If the beam energy is increased in steps, the layer giving maximum yield is located at increasing depths. Proton-induced reactions at 872 keV in F and 992 keV in Al are two examples that have been used for depth profiling. An important application is the use of higher energy ^{7}Li, ^{15}N, or ^{19}F beams for measuring the depth profiles of H in near-surface layers [Tirira et al, 1996].

G. PARTICLE EMISSION

Many nuclear reactions result in the emission of high-energy ions or neutrons [high Q values in Eq. (1)]. For example, (d,p) reactions - an incident deuteron is absorbed and a proton emitted - in ^{12}C, ^{14}N, and ^{16}O give well-separated peaks in an energy spectrum from a thin layer containing these elements. A thin absorber is placed in front of the proton detector to remove low-energy scattered ions. For thicker layers, each peak is extended to lower energies and can be used to derive depth profiles in a similar manner to that described for RBS spectra (Fig. 2). Other examples are (p, α) reactions in ^{15}N, ^{18}O, and ^{19}F, which can be used for depth profiling these isotopes. Neutron emission can also be used, for example, to profile ^{2}D, ^{13}C, ^{15}N, and ^{18}O, but there have been only limited applications of this aspect of IBA [Bird and Williams, 1989].

H. ACTIVATION

The products of ion-induced activation can be used in a similar manner to the better known neutron activation analysis (NAA). Ion energies of 3 to 10 MeV, or even higher, are needed to obtain good yields. Sensitivities down to 1 ng g^{-1} can be achieved for a different suite of isotopes to those for which NAA is most sensitive. A special feature of ion activation is that it is restricted to a surface layer, usually less than 1 mm thick, with the bulk of the sample remaining free of radioactivity. Thin-layer activation is valuable for studying processes such as surface wear [Tesmer and Nastasi, 1995].

III. Applications

The most extensive application of IBA has been in the research and development of advanced materials - particularly semiconductors involving special surface and near-surface properties. A second area of major importance has been the study of contamination, pollution, and other trace element problems. The potential of IBA for making valuable contributions to geo-science and minerals, bioscience and medicine, archeology, and art is well established, so that these and other analytical applications can be expected to expand rapidly. Sequential measurements using different techniques can often be replaced by simultaneous measurements [Cohen, 1993], for example, of RBS, PIXE and PIGME or RBS, ERA, PIXE, and channeling. Depending on the nature of the sample, a selection of high-energy IBA techniques can give a total major element analysis as well as concentrations of a number of trace elements. Facilities have also been developed for carrying out both low-energy and high-energy IBA in the one-sample chamber, which may also be connected to an ion implanter to study implantation effects.

Well characterised neutron beams free of γ-rays are an important tool for radiobiological studies such as DNA damage mechanisms in cells by MeV neutrons [Singh et al, 1985]. A 3 MV light ion accelerator with high current capability is an ideal tool for the production of medium flux neutron beams of

known energies with low γ-ray contamination. These machines can provide neutron fluxes up to $3x10^8$ $ncm^{-2}s^{-1}$ at well characterised neutron energies from a few tens of keV to 6 MeV. Dose rates of around 50 Gy/ hr can be routinely produced from mono-energetic neutron beams of 5.4 MeV from the $^2D(d,n)^3He$ reactions [Dytlewski, 1990]. Dose rates up to 150 Gy/ hr are possible using a deuterium gas target at three atmospheres and deuteron beams of around 30 μA with γ-ray contamination reduced to less than 5% of the total dose.

The unique contributions of IBA methods to the characterisation of thin films, surfaces and interfaces have been appreciated internationally for decades. This application has been well documented in the International Conference on IBA series held every two years since 1973 [IBA, 1998]. More recently several international groups have used their access to high energy heavy ion accelerators to perform heavy ion recoil time of flight (RToF) experiments using energetic heavy ion beams such as 100 MeV iodine [Whitlow et al, 1991; Martin et al, 1994].

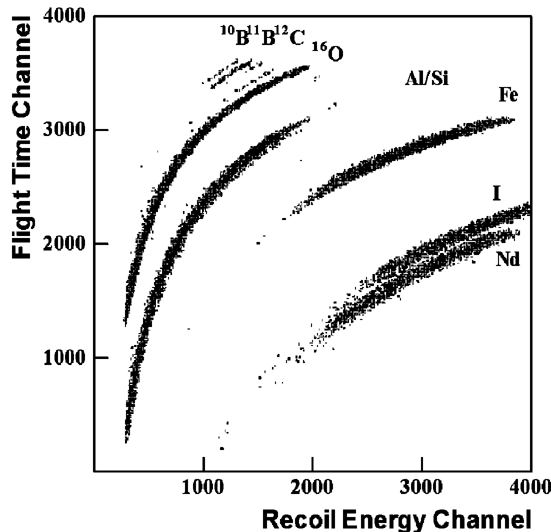

Fig. 7 RToF spectrum of thin layer of FeNdB on silcon using 77 MeV iodine beams

These beams have been used to study a variety of thin metalised films on GaAs and reactions in metal-III-V semiconductor systems in order to develop more stable electrical contacts to these materials [Hult et al, 1995]. Most films and multi-layers studied were typically only a few hundred nanometres thick. Fig. 7 shows a 2 dimensional RToF spectrum for 500nm thick FeNdB film on a silicon wafer. The experiment is to determine the depth profile and concentration of the oxygen contaminant in these films. These data are readily obtainable from the oxygen boomerang shown in Fig. 7.

Low- and high-energy ion microprobes offer a versatility in analysis that is an important addition to the capabilities of other techniques, such as the electron microprobe. One example, shown in Fig. 8, is the elemental distribution in a single grain of sand obtained from PIXE data recorded with a scanning heavy ion microprobe with resolution of about 10 μm.

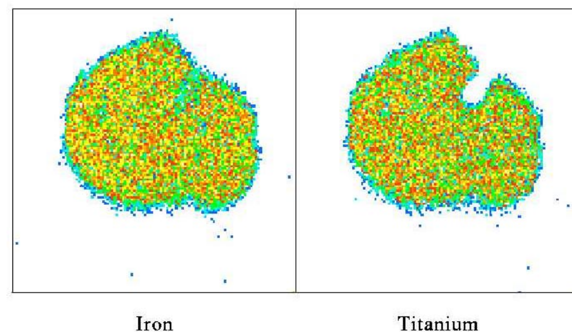

Fig. 8. The elemental distribution in a single grain of sand measured with a scanning heavy ion microprobe [Siegele et al, 1999].

The mineral grain was scanned over an area of about 300x300 μm and the ion beam used to generate the X-rays was a 25 MeV C^{4+} beam. The complete set of recorded data (radiation intensity versus time) can be used to full advantage with computer graphics and spectrum processing to explore spatial or time distributions of a specific element or isotope, the element distribution at a specific location, or any time-dependent changes in element distributions. It is even possible to obtain three-dimensional distributions using

detected radiation energy to provide depth information.

In summary ion beams techniques are ideally to suited for near surface, thin film and multi-elemental analysis. They have high sensitivity, are fast and efficient and often provide depth profile information. Many of the techniques are quantitative and often non-destructive. The range of ion energies and beam types available today means that they can be tailored to solve particular analytical problems. Currently ion beam analysis is being applied internationally in a very broad range of materials problems and environmental issues.

BIBLIOGRAPHY

Benninghoven. A., Huber, A. M., and Werner, H. W., eds. (1988). "Secondary Ion Mass Spectrometry. SIMS VI." Wiley, New York.

Bird, J. R., and Williams, J. S., eds. (1989). "Ion Beams for Materials Analysis." Academic Press, Sydney, Australia.

Breese M.B.H., Jamieson, D.N. and King, P.J.C. (1996) “Materials analysis using a nuclear microprobe.” John Wiley & Sons Inc., New York.

Chu, W.-K., Mayer, J. W., and Nicolet, M.-A. (1978). "Backscattering Spectrometry." Academic Press, New York.

Cohen, D.D. (1993). *Nucl. Instrum. and Methods,* **B79, p385.**

Cohen, D.D. and Rose, E. K., (1992), *Nucl. Instrum. and Methods,* **B66, p158-190.**

Deconninck, G. (1978). "Introduction to Radioanalytical Physics." Elsevier, Amsterdam.

Duggan, J. L., and Morgan, I. L., eds. (1991). Applications of accelerators in research and industry '90. *Nucl. Instrum. Methods* **B56/57**.

Dytlewski, N., Croal, A., Cohen, D., Katsaros, A., Lavin, M., Singh, S. (1990). *Nucl. Instrum. and Methods,* **A28, p641.**

Feldman, L. C., and Mayer, J. W. (1986). "Fundamentals of Surface and Thin Film Analysis." North-Holland, Amsterdam.

Feldman, L. C., Mayer, J. W., and Picraux, S. T. (1982). "Materials Analysis by Ion Channeling." Academic Press, New York.

Hult, M., Persson, L., El Bouanani, M., Whitlow, H.J., Anderson, M., Östling, M., Lundberg, N., Zaring, C., Georgesson, K., Cohen, D.D., Dytlewski, N., Johnston, P.N., Walker, S.R.. (1995) *J. Appl. Phys.* **77, p2435.**

IBA Proceedings, Lisbon, Portugal, June 1998, *Nucl. Instrum. and Methods,* **B136-138, 1-1367.**

Legge, G. F. J., and Jamieson, D. N., eds. (1991). Nuclear microprobe technology and applications. *Nucl. Instrum Methods* **B54**.

Martin, J.W., Cohen, D.D., Dytlewski, N., Garton, D.B., Whitlow, H.J., Russell, G.J., (1994). *Nucl. Instr. and Methods,* **B94, p277-290.**

Moschini, G. and Valkovic, V. (1996). Particle induced x-ray emission and its analytical applications. *Nucl. lnstrum. Methods* **B109, p1-705.**

Siegele, R., Cohen, D.D., and Dytlewski, N. (1999), *Nucl. Instr. and Methods,* **B158, p31.**

Singh, S., Cohen, D.D., Dytlewski, N., Houldsworth, J., Lavin, M., (1989) in Progr. Biophys. Molec. Biol.

Tesmer, J.R. and Nastasi, M. (1995) “Handbook of Modern Ion Beam Materials Analysis.” Materials Research Society, Pittsburg, 1995.

Tirira, J., Serruys, Y. and Trocellier, P. (1996) “Forward Recoil Spectrometry.” Plenum Press, New York.

Watt, F., Osipowicz, T., Choo, T.F., Orlic, I., and Tang, S.M. (1998). . *Nucl. lnstrum. Methods* **B136-138, p313.**

Whitlow, H.J., Jakobsson B., and Westerberg L., (1991) *Nucl. Instr. and Methods,* **A310, p636-648.**

Vis, R. D., ed. (1990). Particle induced x-ray emission and its analytical applications. *Nucl. lnstrum. Methods* **B49**.